ELSEVIER

Journal of Molecular Catalysis A: Chemical 193 (2003) 259–272

JOURNAL OF MOLECULAR CATALYSIS A: CHEMICAL

www.elsevier.com/locate/molcata

# Propene hydroformylation by supported aqueous-phase Rh-NORBOS catalysts

A. Riisager [a], K.M. Eriksen [a], J. Hjortkjær [b], R. Fehrmann [a,*]

[a] *Department of Chemistry, Interdisciplinary Research Center for Catalysis, Technical University of Denmark, DK-2800 Lyngby, Denmark*
[b] *Department of Chemical Engineering, Interdisciplinary Research Center for Catalysis, Technical University of Denmark, DK-2800 Lyngby, Denmark*

Received 3 April 2002; accepted 8 August 2002

**Abstract**

The gas-phase hydroformylation reaction of propene using supported aqueous-phase (SAP) Rh-NORBOS modified catalysts in a continuous flow reactor has been examined. SAP catalysts supported on six different support materials were made by wet impregnation using solutions of the precursor complex $Rh(acac)(CO)_2$ and NORBOS ligand. Catalytic performance of silica gel-based catalysts was examined by altering catalyst composition and reaction conditions. Results were compared to analogous TPPTS catalysts and to catalysts supported on alternative support materials, e.g. silica glass, alumina and carbon. Based on these results the aqueous and the homogeneous nature of the SAP catalysts are discussed.


*Keywords:* Hydroformylation; Supported aqueous-phase; Rhodium; NORBOS; Propene

## 1. Introduction

It is well recognized that immobilization of homogeneous catalysts constitute a class of catalysts which can combine the advantages of classical heterogeneous and homogeneous catalysis, i.e. high chemoselectivities and mild reaction conditions with ease of catalyst separation and recycling [1]. Despite this, there is to our knowledge yet no successful commercialization of a solid catalyst that is an immobilized homogeneous catalyst. The reasons for this are usually explained by low activity, low selectivity, and leaching of the active component [2].

In the late 1980s the novel catalytic concept termed supported aqueous-phase catalysis (SAPC) was developed as a candidate for performing interfacial immobilized catalysis [3]. The technique involves absorption of an aqueous solution of a catalytic active organometallic complex onto a high-surface area hydrophilic support material. So when performing, e.g. hydroformylation reactions, using lipophilic organic substrates—liquid or gaseous—reactions takes place preferentially at the aqueous–organic interface due to the low solubility of olefins in water (0.5–0.0005 mol.% for $C_3$–$C_9$ olefins [4]) rather than homogeneously in the supported film as is the case with supported liquid-phase (SLP) catalysts [1]. The separation of phases both during and after catalysis thereby makes catalyst recovery and reuse easy.

The large support surface area ensures a high interfacial area between catalytic species and the reactants

* Corresponding author. Tel.: +45-4525-2389; fax: +45-4588-3136.
*E-mail address:* rf@kemi.dtu.dk (R. Fehrmann).

1381-1169/02/$ – see front matter 
PII: S1381-1169(02)00471-5

thereby compensating for mass-transfer limitations. Water-solubility of the complex is obtained by introducing hydrophilic groups like, e.g., $-SO_3^-$, $-CO_2^-$ or $-NH_4^+$ [5–10], or more recently also $-PO_3^{2-}$ ([11] and references therein), to the coordinated ligands.

The SAPC immobilization concept has shown to be effective for many metal ion catalyzed reactions in reaction media immiscible with water [2,12,13]. Most of these are concerned with olefin hydroformylation reactions. The hydroformylation reaction using Rh-based catalysts was also used primarily to obtain proof of the concept [3,14–16]. Hydroformylations using SAPC have since then, beside the continuous use of Rh-complexes [17–28], also been extended to include use of transition metal complexes of Pt [23,29] and Co [23,30,31]. However, since the activity with regard to the central metal atoms follows the order: Rh ≫ Co ≫ Pt [8], the main focus continuous to concentrate on use of rhodium.

Most of the Rh-SAPC hydroformylation applications have been limited to the use of tris(*m*-sulfonatophenyl)phosphine, TPPTS (**1**), as ligand (Scheme 1). Exceptions are the bidentate sulfoxantphos (**2**) ligand [22] and the hexDPPDS (**3**) ligand [23] used for hydroformylation of 1-octene and $C_8$–$C_{12}$ olefins, respectively. They are modified as TPPTS with sulfonate groups. When using sulfonated ligands the hydrophilicity of the ligands and the support creates interaction energies sufficient to maintain the immobilization during and after reaction. Hydrogen bonding between hydrated alkali metal-sulfonate groups and the surface is generally accepted as causing the immobilization [19].

It is therefore not surprising that the catalytic performance of SAP catalysts have a very strong dependence on the hydration rate of the support. This has been shown for many reaction systems using sulfonated ligands, e.g. the hydroformylation of 1-heptene utilizing $HRh(CO)(TPPTS)_3$/CPG catalyst [16], where differences in catalyst activity of $10^2$ were observed between dry and hydrated catalysts. Catalyst regioselectivity did also vary with support hydration rate and was ascribed as reflecting a significant change in the catalytic pathway. In 1-octene hydroformylation using $[Rh_2(\mu\text{-}S^tBu)_2(CO)_2(TPPTS)_2]$/silica an opti-

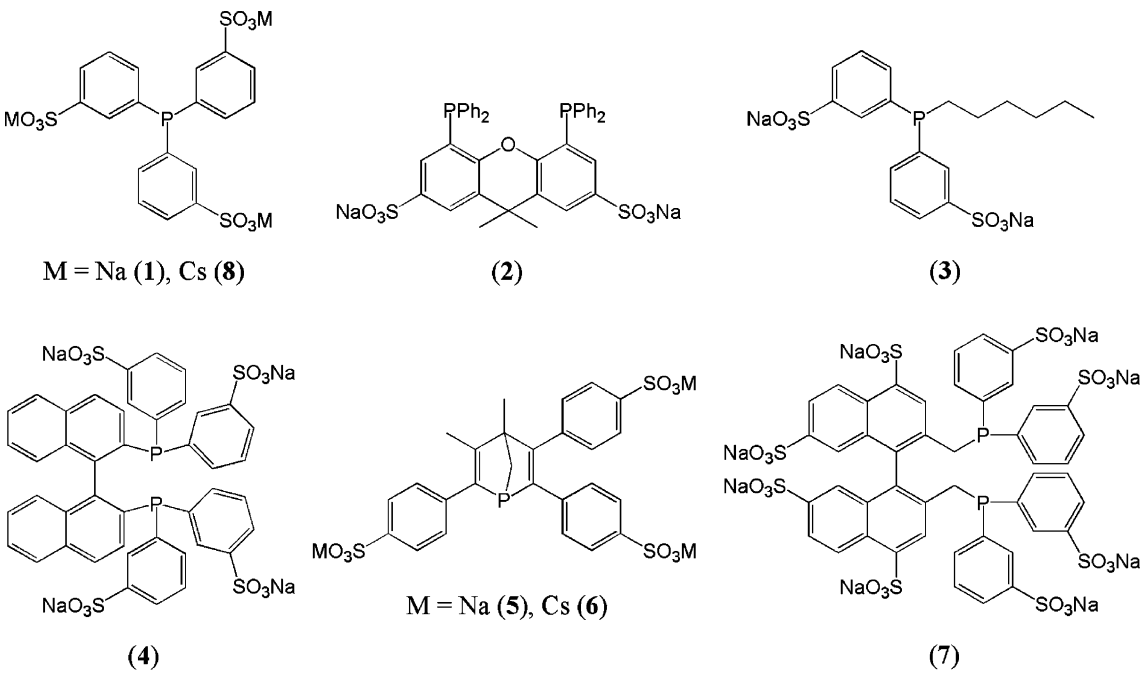


Scheme 1. Water-soluble sulfonated phosphine ligands: (**1**, **8**), TPPTS; (**2**), sulfoxantphos; (**3**), hexDPPDS; (**4**), BINAP, (**5**, **6**), NORBOS; and (**7**), BINAS-8.

mum activity was observed in a very narrow hydration range, corresponding to one to two water monolayers covering the support surface [25,32]. Likewise, in the Wacker oxidation of 1-heptene using $PdCl_2$-$CuCl_2$/CPG catalysts [33], asymmetric hydrogenations using [Ru(benzene)(BINAP)Cl]Cl/CPG catalyst [34] (BINAP, **4**) and allylic alkylation (Trost–Tsuji reaction) using a $Pd(OAc)_2$-TPPTS/silica catalyst [35] were analogous catalyst activity versus hydration relations found. All these studies lead recently to the confirmation that pore sizes and hydration rate of the support are the key factors in SAPC [36].

Recently, it has been reported that the phosphine ligands tri-sodium 3,4-dimethyl-2,5,6-tris(*p*-sulfonatophenyl)-1-phosphanorbornadiene (NORBOS) (**5**) [37] and octa-sodium 2,2′-bis[di(*m*-sulfonatophenyl)phosphinomethylen]-4,4′,7,7′-tetrasulfonato-1,1′-binaphthalene (BINAS) (**7**) [37,38] (Scheme 1) have shown superior activity compared to TPPTS in the Rh catalyzed biphasic hydroformylation of propene. This discovery, combined with the advantages using the SAP approach, has therefore lead us to initiate a closer investigation of hydroformylation reactions using these ligands in SAP catalysis.

In the study reported here NORBOS ligand modified Rh-complexes are used as SAP catalysts in the hydroformylation of propene using a continuous flow mode. A multifactorial analysis based on reaction kinetics with respect to catalyst performance has been performed, and the effects of changing reaction and catalyst parameters such as temperature, pressure, feed gas composition, ligand-to-rhodium ratio, and support material are discussed. Further, the physical state of the aqueous catalytic-phase of the SAP catalyst during reaction conditions is discussed, and arguments pointing to a heterogeneous character of the SAP concept are put forward.

## 2. Experimental

### 2.1. General comments

Solvents used for ligand and SAP catalyst synthesis were degassed by reflux for several hours under inert gas (nitrogen or argon) prior to use. All manipulations were done using standard Schlenk and syringe techniques under argon gas.

2,3-Dimethylbutadien (98%), dichlorophenylphosphine (97%), diphenylacetylene (98%), and Rh(acac)$(CO)_2$ (98%) were purchased from Aldrich. Fuming sulfuric acid (30% $SO_3$), silica gel 100 and aluminum oxide 90 activity neutral from Merck, CPG-75 and CPG-2000 from Sigma, and carbon CABOT XC-72 from Vulcan. Industrial catalyst support based on kiselguhr, HT1, was obtained from Haldor Topsøe A/S. Prior to use CABOT XC-72 support was cleaned for sulfur and made hydrophilic by heating in Formier gas (1100 °C, 36 h) followed by 3 M $H_2O_2$ treatment (50 ml/g cat, 25 °C, 16 h). All other materials were used as received.

For hydroformylation reactions propene (99.4%), carbon monoxide (99.997%), and hydrogen (99.9997%) purchased from Hede Nielsen A/S were used without further purification. Product analysis was performed on a Shimadzu GC-9A gas chromatograph equipped with a Nukol™ capillary column (15 m × 0.53 mm ID, Supelco Inc.). Detection was done by flame ionization using standard grade nitrogen, hydrogen and technical air. *n*-Butanal (99%) and *iso*-butanal (>98%) from Aldrich, and *iso*-propanol (Merck) used for GC calibrations were distilled prior to use. All other reagents and solvents used were of analytical grade.

FT-IR spectra were recorded on a Perkin-Elmer 1710 FT-IR spectrophotometer using KBr tablets. pH values were measured with a Radiometer PHM62 pH meter using a combined glass electrode (Radiometer). Liquid NMR spectra were recorded on a Varian VXR 300 MHz spectrometer in $D_2O$ at 25 °C ($^1$H-NMR: 300 MHz. $^{13}$C $\{^1H\}$-NMR: 50.323 MHz, both referenced to external TMS. $^{31}$P $\{^1H\}$-NMR: 121.474 MHz, referenced to external 85% $H_3PO_4$). $^{29}$Si CP-MAS NMR spectra were recorded on an INOVA 400 MHz spectrometer with SPARC system ($^{29}$Si $\{^1H\}$-NMR: 79.436 MHz).

### 2.2. Ligand preparation and characterization

The tri-sodium salt of the NORBOS ligand, NORBOS-$Na_3$ (**5**), was prepared in a three step synthetic procedure described in the literature [37,39,40]. Virtually oxide free (**5**) was obtained from the crude product upon purification by analytically RP-HPLC on a Radial-Pac™ Cartridge 8NVC-18-6 column (Waters) operated at RT with a mobile-phase of 5%

acetonitrile in water at a flow rate of 1.5 ml/min using an evaporative light scattering detector ($\lambda = 280$ nm). The identity and purity of (**5**) was confirmed using NMR ($^{1}$H, $^{13}$C and $^{31}$P) and IR spectroscopy.

The tri-cesium salt of NORBOS (**6**) was prepared in an analog way to (**5**), using 5% CsOH solution in the final neutralization step instead of NaOH. Both NMR and IR data of (**6**) were identical with the data of (**5**). More details on the synthesis and further characterization of (**6**) will be reported elsewhere.

Tri-cesium tris(*m*-sulfonatophenyl)phosphine, TPPTS-$Cs_3$ (**8**), was made by a similar modification as above of a literature method describing the synthesis of TPPTS-$Na_3$ [41].

### 2.3. Preparation and characterization of SAP catalysts

NORBOS and TPPTS-$Cs_3$ ligand modified SAP catalysts were prepared using silica gel, CPG, alumina, carbon and HT1, respectively, as support materials. All catalysts were made to have a initial rhodium content of 2 mg Rh per g support (0.2 wt.% Rh). Preparations followed a general biphasic impregnation procedure here illustrated for SAP-Si3a (molar ratio P/Rh = 2.85): 20.0 mg of Rh(acac)$(CO)_2$ (0.078 mmol) and 148.6 mg NORBOS-$Na_3$ (**5**) (0.221 mmol) where dissolved in 10 ml water/dichloromethane (50:50) vol.% under vigorously magnetic stirring. After 30 min the stirring was slowed down and 4.0 g silica gel was suspended in the mixture. After further stirring for 2 h the solvent mixture was slowly removed under reduced pressure (≈30 Torr) at 35 °C on a Heidolph rotatory evaporator equipped with water aspirator and waterbath at a revolution speed of 100 rpm. Finally, the resulting catalysts were dried in vacuo at 110 °C overnight to remove the last adsorbed water and stored in vacuo over $P_4O_{10}$ prior to use.

Contents of rhodium in the catalysts were determined by atomic absorption spectroscopy (AAS) on a Perkin-Elmer 2100 AA spectrophotometer. Solutions were made by stirring the catalysts in 6 M aqua regia for 20 h at 50 °C followed by dilution. Water contents were determined by thermogravimetric analyses (TGA) on a Mettler TA1 NT instrument under constant nitrogen gas flow (87 ml/min). BET surface areas, pore volumes and pore diameters were determined by $N_2$ adsorption/desorption experiments on a Micromeritics Gemini 2375 instrument.

### 2.4. Continuous propene hydroformylation using SAP catalysts

The gas-phase propene hydroformylation reactions were studied using a microcatalytic flow system where the SAP catalysts formed a short bed in a stainless steel tubular reactor, essentially as described in [42]. Analysis of the product composition was performed using FID-GC by periodically injecting sample into the column via a sample loop and a splitter valve. Outlet gas flow from the reactor were measured continuously with a HP Electronic flowmeter calibrated to the feed gas using a Chrompack Optiflow 520 digital flowmeter. GC calibration was performed prior to catalytic measurements using solutions of *n*- and *iso*-butanal (purity confirmed by $^{1}$H-NMR) in *iso*-propanol.

A general procedure for a catalytic measurement involved following steps. About 50 mg SAP catalyst was placed in the reactor. A water saturated premixed feed gas of $C_3H_6$:CO:$H_2$ was flushed through the system for 1 h at 5.0 atm, whereafter the reaction was started by lowering the reactor into a thermostatic preheated oil bath (Lauda Thermostat, ±1 °C). The feed gas was humidified in a thermostatic stainless steel water tank (±1 °C) before entering the reactor. The water content in the humidified feed gas can be changed by varying the water tank temperature, and calculated using Raoults law and Antoine's equation assuming ideal gas behavior.

The feed gas flow was adjusted to maintain a differential conversion of propene (approximately 1%) resulting in GHSV of 10.000–20.000 $h^{-1}$ corresponding to contact times of 0.18–0.36 s. This allowed calculation of the turn over frequency (TOF) for *n*- and *iso*-butanal formation, respectively, as $F$[aldehyde]/$W_{Rh}$ where $F$ is the gas flow (ml/s) from the reactor, [aldehyde] is the concentration of *n*- or *iso*-aldehyde (mol/ml) in the product stream and $W_{Rh}$ is the weight of rhodium in the reactor. Since no by-products, e.g. from hydrogenation or aldol condensation, were observed during reactions the overall rate of the hydroformylation reactions were the sum of the rates for *n*- and *iso*-butanal formation. The regioselectivity is defined as the ratio between the rates of *n*- and *iso*-butanal formation (*n*/*iso* ratio).

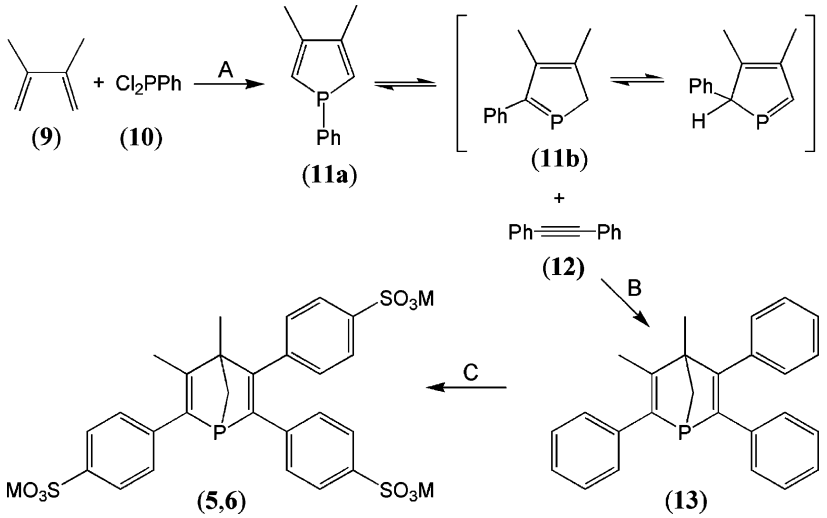


Scheme 2. Synthetic pathway for NORBOS-$M_3$ (M = Na (**5**), Cs (**6**)). (Reaction A) 25 °C, 12 days then 2-picoline, 25 °C, 48 h (76%). (Reaction B) *o*-xylene, reflux, 72 h (59%). (Reaction C) (**5**): 30% oleum, 5 °C, 45 min then 3 M NaOH (69%); (**6**): 30% oleum, 5 °C, 45 min then 3.8 eq. tri-isooctylamine in toluene then 1 M CsOH then 3 M $H_2SO_4$ (50%).

## 3. Results and discussion

### 3.1. Ligand synthesis and characterization

The first step in the synthesis of NORBOS involved the preparation of 3,4-dimethyl-1-phenylphosphole (**11**) [39] (Scheme 2). Starting from 2,3-dimethylbutadien (**9**) a McCormac cyclo addition reaction [43] of dichlorophenylphosphine (**10**) followed by base promoted dehydrochloronation gave the 1H-phosphole (**11a**). In the second step reported by Mathey et al. [40] Diels–Alder [4 + 2] cyclo addition reaction of phosphole with diphenylethyne (**12**) gave 3,4-dimethyl-2,5,6-triphenyl-1-phosphabicyclo-[2,2,1]-heptadiene (**13**) by reaction with the isomeric 2H-phosphole (**11b**) formed by [1,5] sigmatropic phenyl-hydrogen shifts from (**11a**). Finally, the sulfonation procedure of (**13**) with fuming sulfuric acid (30% $SO_3$) [37] gave NORBOS contaminated with approximately 10% of the corresponding phosphine oxide. For both NORBOS-$M_3$ ligands (**5**) and (**6**), the measured NMR data were identical to the data previously reported [37]. Judging from the $^{31}$P-NMR data the oxide levels of both (**5**) and (**6**) were less than 1% of the resulting ligand after RP-HPLC purification and recrystallization, respectively.

Likewise, the NMR data recorded of the prepared TPPTS-$Cs_3$ ligand (**8**) was consistent with the data reported previously [44] and the oxide contamination <1%. In contrast to the preparation of the tri-sodium salt [41], no mono- or di-sulfonated product was observed in the recrystallized cesium salt. Therefore, no further purification step like, e.g. gel permeation chromatography used for purification of TPPTS-$Na_3$, was necessary. Combining the observations it seems like the differences in solubility between the cesium phosphines relative to the corresponding phosphine oxides in methanol/water mixtures can be used to selectively crystallize the phosphines. This is not the case with the sodium salts where contamination seems unavoidable and tedious to remove [41].

### 3.2. Catalyst synthesis and characterization

Silica gel supported SAP catalysts were prepared using the ligands (**5**), (**6**) and (**8**). CPG, alumina, carbon and HT1 supported catalysts were made using (**6**). The catalysts were all obtained as dry powders, which were yellow-colored compared to the free support material (except for the carbon catalysts). The yellow color of the catalysts remained unchanged in most cases after the catalysts had been used, but for

Table 1
Characteristics of supports

| | Silica gel 100 | CPG-75 | CPG-2000 | Alumina 90 neutral | CABOT XC-72 | HT1 |
|---|---|---|---|---|---|---|
| BET surface ($m^2$/g) | 297.5 | 152.7[a] | 11.3[a] | 103.1 | 171.6 | 2.2 |
| Pore volume (ml/g)[b] | 1.015 | NA | NA | 0.253 | 0.886 | 0.007 |
| Total porous volume (ml/g) | 1.015 | 0.47[a] | 0.86[a] | NA | 0.767 | NA |
| Mean pore diameter (Å) | 137 | 74[a] | 1932[a] | NA | NA | NA |
| Particle sizes (μm)[a] | 63–200 | 18–125 | 75–125 | 63–200 | NA | NA |
| Water content (%) | 2.5 | NA | NA | 4.0 | 0.1 | NA |
| pH (5 wt.% in water) | 7.4 | 7.4 | 7.7 | 7.4 | 5.8 | 10.0 |

[a] Data from supplier.
[b] For pores with $d < 500$ Å.

catalysts with low P/Rh ratios (≤2) an initial brownish discoloring did appear over time. The presence of dispersed rhodium metal particles causing the coloring could not be detected by powder XRD, and since the original color was gradually regained upon prolonged storage (in vacuo) the discoloring was attributed to an reversible reaction of the immobilized Rh species due to adsorption of reaction products. Reproducibility of the catalytic performance for the catalysts in consecutive catalytic runs supports this assumption.

CP-MAS $^{29}$Si $\{^1$H$\}$-NMR spectra were recorded of pure silica gel and of the catalyst SAP-Si4 (P/Rh = 3.78, Table 2) prior to and after use in catalysis. The characteristic Si signals corresponding to $Si(OSi)_4$, $Si(OSi)_3OH$ and $Si(OSi)_2(OH)_2$ sites [45], respectively, located at approximately $\delta = -110$, $-100$ and $-90$ ppm were integrated and compared. For silica gel the ratio $[Si(OSi)_4]$:$[Si(OSi)_3OH]$:$[Si(OSi)_2(OH)_2]$ = 5:70:25 was found. For the SAP-Si4 catalyst analog ratios, 4:58:38 and 3:54:43, were found before and after reaction, respectively. Evidently, no significant alternations in the surface Si coordination were observed with the catalyst prior to and after reaction. In contrast, the initial immobilization of the precursor reagents on the silica gel enhanced the more hydrated $Si(OSi)_2(OH)_2$ sites compared to the $Si(OSi)_3OH$ sites as expected, leaving the amount of bulk Si sites unaffected.

Some general physical characteristics of the support materials and of representative catalysts are collected in Tables 1 and 2, respectively.

Table 2
Data for the SAP catalysts

| Catalyst | Ligand no. | P/Rh ratio[a] (mol/mol) | Rh loading[a] (mg Rh/g support) | Rh content[b] (mg Rh/g catalyst) | BET surface[c] ($m^2$/g) | Porous volume[c] (ml/g) |
|---|---|---|---|---|---|---|
| SAP-Si0 | – | 0.00 | 2.000 | 0.858 | 254.6 | NA |
| SAP-Si1 | **5** | 0.94 | 2.000 | 1.158 | 289.7 | NA |
| SAP-Si2 | **5** | 1.89 | 2.000 | 1.283 | 291.2 | NA |
| SAP-Si3a | **5** | 2.85 | 2.001 | 1.445 | 278.3 | NA |
| SAP-Si3b | **6** | 2.85 | 2.000 | 1.284 | 272.9 | 0.939 |
| SAP-Si4 | **5** | 3.78 | 2.000 | 1.578 | 274.2 | NA |
| SAP-Si5 | **5** | 4.73 | 2.000 | 1.305 | 261.2 | NA |
| SAP-Si6 | **5** | 6.63 | 2.000 | 1.174 | 256.4 | 0.883 |
| SAP-Si7 | **5** | 9.47 | 2.000 | 1.148 | 250.4 | 0.834 |
| SAP-Si8 | **8** | 2.85 | 1.999 | 1.668 | 280.6 | NA |
| SAP-CPG75 | **6** | 2.85 | 2.002 | 1.383 | 146.9 | NA |
| SAP-CPG2000 | **6** | 2.86 | 2.001 | 1.460 | 8.5 | NA |
| SAP-Al | **6** | 2.86 | 1.998 | 1.528 | 85.8 | 0.194 |
| SAP-C | **6** | 2.85 | 2.000 | 0.399 | 129.2 | 0.659 |
| SAP-HT1 | **6** | 2.85 | 1.996 | 1.740 | 2.3 | 0.009 |

[a] A priori.
[b] Determined with Rh-AAS.
[c] After drying in vacuo (110 °C, 24 h). For pores with $d < 500$ Å.

The support materials are all mesoporous. Beside this common feature it is clear that characteristics such as BET surface areas, porosity, pore distributions, acidities and hydrophilicities varies for the materials (Table 1). For this reason it was anticipated that the presence of a support dependence on the hydroformylation performance of the SAP catalyst should become very evident when the different materials were used.

The BET areas of the supported catalysts were lower with all support materials than the areas obtained for the pure support (Table 2). In case of the SAP-Si catalysts the areas dropped slightly going to higher P/Rh ratios where increasing amounts of ligand were added. The same trend was observed for the pore volumes where a linear decrease in porosity was observed as a function of the P/Rh ratio. Since the rhodium content was essentially constant in all the catalysts the relation reflects linearity between porosity and added ligand.

The distribution of pores within the different supports was very different. Silica gel had a rather narrow distribution with pores only in the 50–160 Å range and a mean diameter of 137 Å. The silica controlled pore glasses (CPGs) had very narrow pore size distributions (±7%) with mean diameters of 74 and 1932 Å, respectively. Alumina had 75% of its pores within the 25–100 Å range and about 10% >500 Å, carbon had essentially only large pores >200 Å, and HT1 had few pores <100 Å (10%) and about 50% >500 Å. The pore distribution between all the supports and the derived supported catalysts were essential the same before and after impregnation, indicating there is no pore size preference for the adsorbate during impregnation. So, the rhodium species seem to be homogeneous distributed in all the pores of the prepared SAP catalyst.

### 3.3. Propene hydroformylation using SAPC

#### 3.3.1. Influence of the P/Rh ratio and the ligand

The reaction rates (activities) and the selectivities for the hydroformylation of propene to butanals using the SAP-Si-(**5**) catalysts with P/Rh ratios between 0 and 10 at temperatures 80–120 °C are shown in Figs. 1 and 2, respectively. By plotting the activities for each catalyst at the three temperatures in an Arrhenius plot, the overall reaction activation energy ($E_a^r$) could be calculated as the slope of the linear regression line through the data points by assuming $E_a^r$ to have a constant value in the measured temperature range (Fig. 3). In Table 3 additional data for the SAP-Si3 catalysts containing ligand (**6**) and (**8**) are reported.

Under the reaction conditions, $p = 5.0$ atm of partial pressure ratios $C_3H_6$:CO:$H_2$:$H_2O$ = 3:3:3:1, the SAP-Si-(**5**) catalysts showed a maximum rate for aldehyde formation of 0.368 mmol butanal/(s g Rh) at 120 °C at P/Rh = 2.85. In comparison the SAP-Si-(**8**) catalyst (Table 3, entry 5), containing the TPPTS ligand used for commercial propene hydroformylation in the Ruhrchemie/Rhône-Poulenc process (RCH/RP

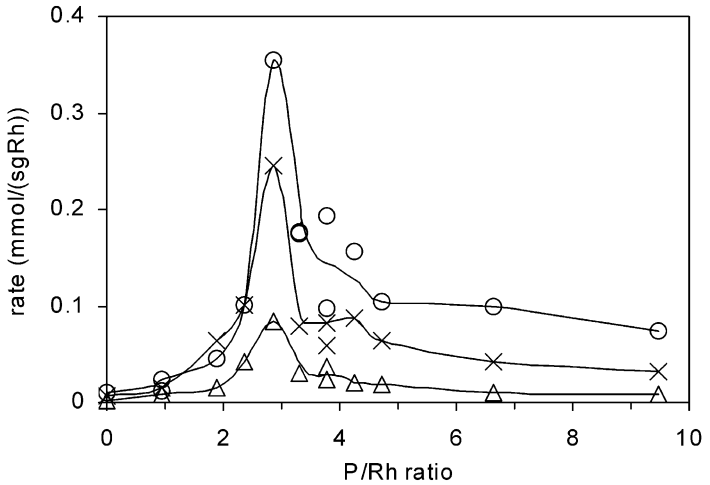


Fig. 1. Propene hydroformylation rates vs. P/Rh ratios and temperature using SAP-Si-(**5**) catalysts: (△) 80 °C, (×) 100 °C, (○) 120 °C, ($p = 5.0$ atm, gas composition CO:$H_2$:$C_3H_6$:$H_2O$ = 3:3:3:1).

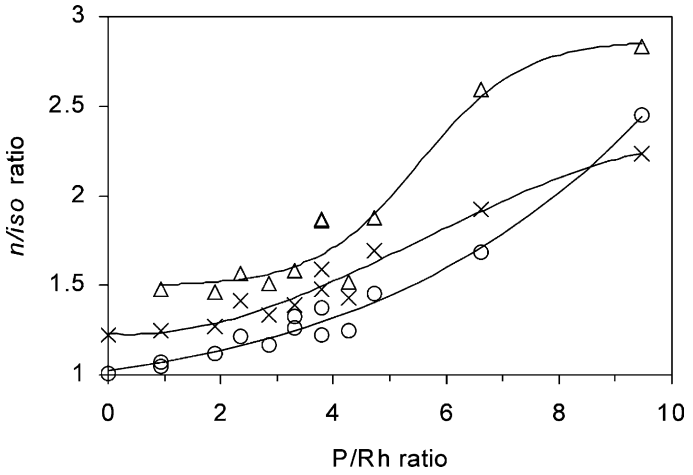


Fig. 2. Selectivity in propene hydroformylation vs. P/Rh ratios and temperature using SAP-Si-(**5**) catalysts: (△) 80 °C, (×) 100 °C, (○) 120 °C, ($p$ = 5.0 atm, gas composition $CO:H_2:C_3H_6:H_2O$ = 3:3:3:1).

process) [46], had an activity 31% lower than the NORBOS-based catalyst measured at the same conditions. From Table 3 it is also clear that substituting sodium by cesium as cation in the NORBOS ligands had no influence on the performance of the catalysts at optimum conditions (entries 1 and 4). The activities were strongly dependent on the P/Rh ratios and showed maxima at all temperatures in a narrow ligand-to-rhodium ratio interval around 3. At P/Rh ratios of about 2 the activity increased steeply before reaching the maximum, and in the range of P/Rh ratios higher than 3 the activity at all temperatures decreased until an activity plateau was reached at P/Rh ≥5.

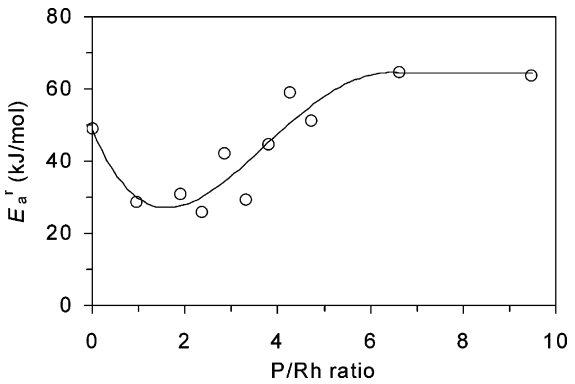


Fig. 3. Calculated reaction activation energies ($E_a^r$) vs. P/Rh ratios using SAP-Si-(**5**) catalysts. ($p$ = 5.0 atm, gas composition $CO:H_2:C_3H_6:H_2O$ = 3:3:3:1).

The observed activity changes at various P/Rh ratios are most likely due to a combination of different effects. When 0 < P/Rh < 3 only gradually enough ligand is available to form active coordinately unsaturated 16 electron complexes, i.e. $HRh(CO)_2$NORBOS and $HRh(CO)(NORBOS)_2$. At P/Rh >3 the activity decline is attributed to a high degree of formation of the saturated $HRh(CO)(NORBOS)_3$ complex, which is the precursor state of the catalyst at higher P/Rh ratios. An analog complex is also readily formed under synthesis gas in the TPPTS system at high P/Rh ratio [47]. Due to lack of free coordination sites it is unable to perform in hydroformylation, and dissociation of phosphine ligand is therefore a prerequisite for catalytic activity when having this complex. At high P/Rh ratios dissociation is inhibited to some extent leading to lower catalyst activity. Since the NORBOS ligand is bulky, formation of tetra-substituted NORBOS complexes is very unlikely. This is in analogy with the fact that TPPTS doesn't form complexes with four TPPTS ligands coordinated [47].

The selectivity declined gradually from $n/iso$ = 2.5 at a P/Rh ratio of 9.5 to about 1.1 for P/Rh = 0 with only minor temperature dependence. The observation that both the optimum P/Rh ratio with respect to activity and the selectivity of the reactions are virtually independent of temperature gives strong indications

Table 3
Activity and selectivity data for hydroformylation of propene using SAPC[a]

| Entry | Catalyst | Support material | Ligand no. | Pressure (atm) | Activity[b] (mmol/(s g Rh)) | TOF[b] (1/h) | *n*/*iso* ratio |
|---|---|---|---|---|---|---|---|
| 1 | SAP-Si3a | Silica gel | **5** | 5.0 | 0.368 | 136.3 | 1.04 |
| 2 | SAP-Si3a | Silica gel | **5** | 10.0 | 0.688 | 254.9 | 1.11 |
| 3 | SAP-Si3a | Silica gel | **5** | 14.0 | 0.696 | 257.8 | 1.12 |
| 4 | SAP-Si3b | Silica gel | **6** | 5.0 | 0.357 | 132.3 | 1.12 |
| 5 | SAP-Si8 | Silica gel | **8** | 5.0 | 0.248 | 91.9 | 1.18 |
| 6 | SAP-CPG75 | Glass | **6** | 5.0 | 0.129 | 47.8 | 0.99 |
| 7 | SAP-CPG2000 | Glass | **6** | 5.0 | 0.015 | 5.6 | 1.01 |
| 8 | SAP-Al | Alumina | **6** | 5.0 | 0.497 | 184.1 | 0.96 |
| 9 | SAP-C | Carbon | **6** | 5.0 | 0.118 | 43.7 | 1.36 |
| 10 | SAP-HT1 | Kiselguhr | **6** | 5.0 | 0.011 | 4.1 | 1.53 |

[a] $T = 120\,^{\circ}C$, P/Rh = 2.85, gas composition $CO:H_2:C_3H_6:H_2O = 3:3:3:1$.
[b] Measured at steady-state conversion.

to, that no changes in reactions mechanism or temperature dependent side reactions are occurring in the measured temperature interval. Interestingly, it has previous been reported that the ligand (**5**) in liquid–liquid biphasic rhodium catalyzed hydroformylation of propene showed almost no catalytic activity below 116 °C [37]. From the results obtained here it is obvious that this is not true for the analog SAP-Si catalysts.

The apparent reaction activation energies ($E_a^r$) changes with the P/Rh ratio (Fig. 3). The lowest $E_a^r$ estimated was obtained in the P/Rh range of 2.5–3 close to where the fastest reaction rate was measured, as one would expect. It had a rather low value of about 30 kJ/mol implying mass-transfer limitations. At P/Rh ratios above 5, $E_a^r$ reached a value of ca. 65 kJ/mol and were apparently independent of additional amount of ligand present in the catalyst system. In contrast to the low value, this activation energy is probably related to a true chemical reaction.

### 3.3.2. *Influence of the water content*

The influence of the water content on the most active catalyst, SAP-Si3b catalyst, was examined with respect to activity and selectivity. The results are shown in Fig. 4.

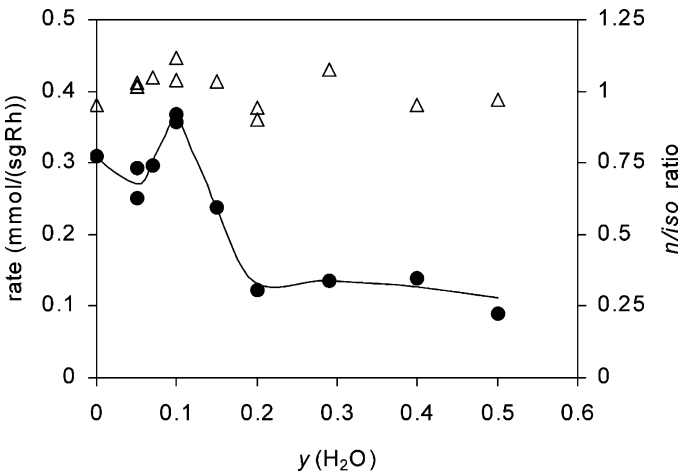


Fig. 4. Performance of the SAP-Si3b catalyst vs. water content in the feed gas: (●) rates, (△) *n*/*iso* ratios. (P/Rh = 2.85, $T = 120\,^{\circ}C$, $p = 5.0$ atm, gas composition $CO:H_2:C_3H_6 = 1:1:1$).

It is clear from Fig. 4 that changes in the water content in the feed gas also induced changes to the catalyst performance. The activity increased when going from a dry feed gas ($y(H_2O) = 0$) through a maximum at $y(H_2O) = 0.10$, which corresponds to $p(H_2O) = 0.50$ atm. At higher water contents, i.e. $y(H_2O) \geq 0.20$, the activity rapidly decreased and a plateau was reached. The *n*/*iso* ratio remained independent of $y(H_2O)$ at a value of approximately 1.0. The observed changes in activity can be explained by reduced surface mobility when $y(H_2O)$ is very low. The increased mobility is most likely due to increased coverage by Si–OH groups on the surface of the support. At high $y(H_2O)$ pore condensation of water can drastically lower the surface area of the catalyst thus decreasing the activity. Furthermore, the catalyst is easily limited by mass transfer limitations due to the very low solubility of the reactants in the aqueous-phase. By using the ideal Kelvin equation and assuming a contact angle of 0° and a surface tension of water at 120 °C of 0.0555 J/cm$^2$, one finds that pore condensation starts around $y(H_2O) \approx 0.3$ with the present supports pore size distribution. This is a slightly higher $y(H_2O)$ than where the activity levels off in Fig. 4, but the Kelvin equation does not take into account surface properties of the support, i.e. acidity and non-ideal shaped pores. Thus, it is reasonable to conclude that the activity plateau at $y(H_2O) > 0.3$ is a direct consequence of catalyst flooding caused by water capillary condensation in the porous structure of the catalyst.

The maximum activity was obtained at $y(H_2O) = 0.10$, but was only slightly higher than under "dry" conditions. So it seems that only a small, but accurate, amount of water is required to optimize the catalyst with respect to activity. Ex situ TGA experiments showed that the water uptake of both the pure silica gel and the SAP-Si3b catalyst are approximately 4 wt.% under conditions where $p(H_2O) = 0.5$ atm. This corresponds to water coverage of the catalyst surface of about 0.4 monolayer, and suggests that water is present as surface hydrates rather than as a liquid-phase during reaction. Water (10 mol.%) in the feed gas is probably just the right amount of water vapor to keep the surface humidified without causing wetting, which eventually leads to pore filling and flooding. Therefore it is also obvious that the active catalytic species mostly behave as heterogenized species with reduces mobility rather than homogeneous complexes, as also prior has been stated and explained by ionic interactions between alkali metal-sulfonate groups and the surface [19]. Other results related to the aqueous nature of the SAP catalyst by Hanson et al. [48] on the mobility of $HRh(CO)(TPPTS)_3$ supported on CPG-240 derived from measuring $^{31}$P-NMR spin lattice relaxation times ($T_1$) doesn't seem to support the conclusions presented here. However, combination of a low surface area (78 m$^2$/g) of the support and very high complex loading (13.2 wt.%) in that study makes the direct comparability questionably, since it is unlikely that the ligand surface titration phenomena seen here could be detected in their study due to surface saturation.

In contrast to the activity the selectivity didn't change with the water contents of the feed gas, but remained at a value of about 1.0 during reactions at all feed gas compositions. This support the conclusions drawn above about the heterogeneous character of the active species, since high selectivity only are anticipated in cases where the mobility of the ligands and the Rh-complexes is high and not for heterogeneous catalyst systems. An example here of is, the before mentioned liquid–liquid biphasic Rh-(**5**) complex catalyzed hydroformylation of propene, where *n*/*iso* ratio of about 4 could be obtained [37].

### 3.3.3. *Influence of the total pressure and p(CO)*

Performance of the SAP-Si3b catalyst upon changes of the total feed gas pressure, *p*, is shown in Table 3. Activities and selectivities obtained with the same catalyst using different gas compositions with various $p(CO)$ and constant $p(C_3H_6)$ and $p(H_2)$ (balanced with argon) as function of reaction temperature are illustrated in Fig. 5.

From Table 3 it is seen that the activity apparently changed linearly with *p* up to about 10 atm. At 14 atm approximately the same activity was observed as the one observed at 10 atm (entries 1–3). The selectivity changed about 10% upon the pressure enhancement (*n*/*iso* = 1.04–1.12). So unsurprisingly, a better performance can be obtained at higher *p*.

When a feed gas with lower CO content was used for reaction with the SAP-Si3b catalyst, the positive effect of higher temperature on the activity became smaller with lower $p(CO)$. At 80 °C no effect of changing the gas composition was observed. The gradual vanishing of temperature effects on the activity was probably due

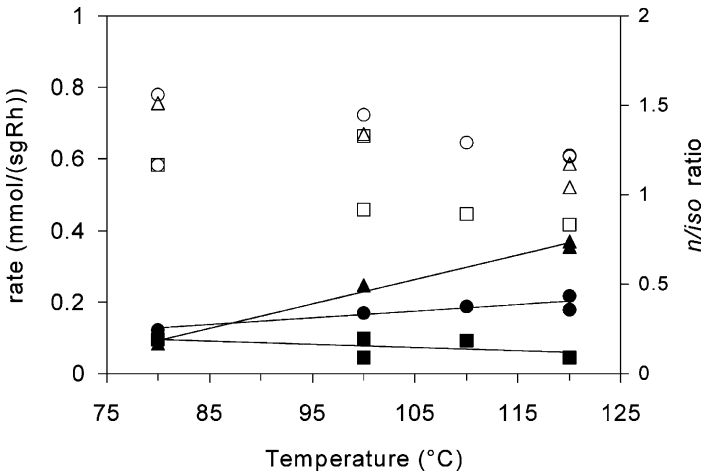


Fig. 5. Performance of the SAP-Si3b catalyst with various feed gas compositions as function of the temperature (filled symbols: rates, open symbols: *n*/*iso* ratios. P/Rh = 2.85, $p = 5.0$ atm, gas compositions $CO:H_2:C_3H_6:Ar:H_2O$: (●) 3:6:6:3:2, (■) 4:12:12:8:4, (▲) 3:3:3:0:1).

to the catalyst suffering from transport limitation of CO gas from the feed gas. With the gas having the lowest CO content, $CO:H_2:C_3H_6:Ar:H_2O = 4:12:12:8:4$, there was no temperature effect observed at all. Therefore, a comparison of estimated reaction activation energies from the data measured with low CO content and those measured at stoichiometric gas compositions are not meaningful. For all three gas compositions a linearly decrease in the *n*/*iso* ratio are observed as function of the temperature as well (Fig. 5).

### 3.3.4. *Influence of the support*

The influence on activity and selectivity by changing the catalyst support material were further examined for the catalyst having P/Rh = 2.85 using ligand (**6**) (Table 3). In Fig. 6, the performance of the silica-based catalyst, SAP-Si3b (silica gel), SAP-CPG75 and SAP-CPG2000 (glasses) and SAP-HT1 (kiselguhr) are shown as function of their BET surface areas.

From Table 3 is it evident that there are large differences in both the activities and selectivities

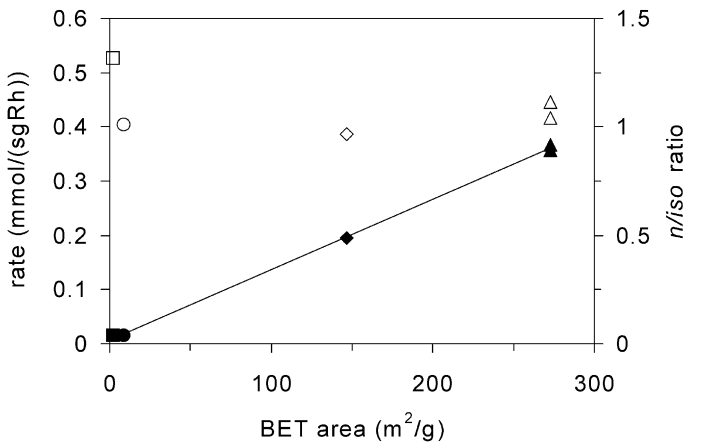


Fig. 6. Activity and selectivity vs. BET areas of silica based catalysts (filled symbols: rates, open symbols: *n*/*iso* ratios. Supports: (■) HT1, (●) CPG-2000, (◆) CPG-75, (▲) silica gel. P/Rh = 2.85, $T = 120\,^{\circ}C$, $p = 5.0$ atm, gas composition $CO:H_2:C_3H_6:H_2O = 3:3:3:1$).

obtained when the support materials are changed. With respect to activity the catalyst follows the order: SAP-Al > SAP-Si > SAP-CPG75 ≈ SAP-C ≫ SAP-CPG2000 ≈ SAP-HT1. Almost the opposite order is found with respect to selectivity with the exception of the SAP-CPG2000 catalyst, which gave about the same selectivity (*n*/*iso* = 1.0–1.1) as the other silica-based catalysts.

It is known from studies of the RCH/RP process that performance of the catalyst is directly influenced by the pH in the aqueous-phase during reaction [46]. From heterogeneously catalyzed hydroformylation it is also generally accepted that variations of the surface of the support, e.g. with respect to acidic sites, have influence on the catalyst performance [49]. Evaluation of pH values measured of 5 wt.% suspensions of the various supports (Table 1) with the activities measured for the catalysts supported onto the particular support material (Table 3, entries 4 and 6–10), gives no definitive indications to the role of support surface acidity. But apparently support surface acidity around pH = 7.5 are optimal for the conditions examined here.

The four silica-based supports have large variations in their surface areas (Table 1), but surfaces that chemically do not differ significant. Therefore, the silica-based catalysts are directly comparable with respect to their catalytic performance.

In Fig. 6 a linear decline are observed between catalyst activity and the surface areas of the different silica-based catalyst, meaning that the catalysts have activity dependencies which are directly proportional to the number of active catalytic species exposed on the catalyst surfaces during reaction. Assuming that the active species are derived from $HRh(CO)(NORBOS\text{-}Cs_3)_3$ with has an estimated projected area of approximately 190 Å$^2$ per molecule [50], a coverage of active species of more than a monolayer is expected when catalysts have surface areas lower than approximately 20 m$^2$/g. Combining this assumption with the observation that a strong surface dependence of the reaction exist, gives proof to that the catalyst is operating in a heterogeneously catalytic mode and not as an immobilized dissolved homogeneous catalyst. Similar arguments has prior been used to establish, e.g. the homogeneous character of the SLP $V_2O_5$ based sulfuric acid catalyst [51].

## 4. Conclusions

Catalytic performance of silica gel-based Rh-NORBOS SAP catalysts was examined by altering the catalysts ligand-to-rhodium ratios (P/Rh ratios) and water contents together with reaction temperature and gas compositions, in the continuous gas-phase hydroformylation of propene. Maximum hydroformylation rate of 0.368 mmol/(s g Rh) (steady state TOF = 136.3 h$^{-1}$) was obtained in a narrow P/Rh interval around 3 with a feed gas having stoichiometric amounts of reactants and a water content of $y(H_2O) = 0.10$ ($T = 120\,^{\circ}C$, $p = 5$ atm, gas composition: $CO{:}H_2{:}C_3H_6{:}H_2O$ = 3:3:3:1). This was approximately 50% higher than analogous catalysts based on TPPTS ligand. The reaction activation energy at optimum conditions was estimated to be about 30 kJ/mol implying mass-transfer restrictions.

With respect to activity the catalysts had a strong dependence of the P/Rh ratio, but were independent of which of the cations, sodium or cesium, that was present as counterion in the NORBOS ligand. Dependence of *p*(CO) at low CO pressures revealed that the catalysts suffered from transport limitation of CO gas from the feed gas. Activity decline observed using water rich feed gas ($y(H_2O) \geq 0.30$) was attributed to capillary condensation of water in the porous structure of the support. The relatively small amount of water needed to reach maximum activity is probably present in the catalysts as a floating monolayer, i.e. surface hydrates, rather than as condensed liquid and is believed to be necessary to ensure a certain mobility of the active species. Therefore, one might suggest that the term "supported aqueous-phase catalyst" is somewhat misleading since no aqueous-phase is present in the catalyst during operation. Experimental evidence rather suggests that the catalyst is heterogeneous with enhanced surface mobility properties.

Comparison of the silica gel catalysts with catalysts supported on alternative support materials established the activity order: alumina > silica > carbon > HT1, with respect to support influence at the optimized conditions used for reactions using the silica-based catalysts. Measurement of support surface acidities indicated that an acidity around pH = 7.5 was optimum for the catalyst performance, even though no clear distinction between the beneficiary effect of

factors such as, e.g. acidity, hydrophilicity and porosity could be made.

In general, low regioselectivities was obtained (*n*/*iso* ratios <3) with all the catalysts. A linear relation was observed between catalyst activity and surface areas of four different silica-based catalysts having Rh complex loadings corresponding to about 0.4–2.4 monolayers. Based on these facts it is probable that the catalysts operate as supported solid-phase catalysts rather than as immobilized dissolved homogeneous catalysts under the reaction conditions examined.

## Acknowledgements

The Danish Technical Research Council has supported this investigation. Haldor Topsøe A/S, Denmark has kindly provided us with the HT1 support.

## References

[1] F.R. Hartley, Supported Metal Complexes, Riedel, Dordrecht, 1985.
[2] M.E. Davis, in: B. Cornils, W.A. Herrmann (Eds.), Aqueous-Phase Organometallic Catalysis, Chapter 4.7, Wiley, Weinheim, 1998, p. 241.
[3] J.P. Arhancet, M.E. Davis, J.S. Merola, B.E. Hanson, Nature 339 (1989) 454.
[4] B. Cornils, W.A. Herrmann, Aqueous-Phase Organometallic Catalysis, Chapter 1, Wiley, Weinheim, 1998, p. 3.
[5] P. Kalck, F. Monteil, Adv. Organomet. Chem. 34 (1992) 219.
[6] W.A. Herrmann, C.W. Kohlpaintner, Angew. Chem. Int. Ed. Engl. 32 (1993) 1524.
[7] B. Driessen-Hölscher, Adv. Catal. 42 (1998) 473.
[8] M. Beller, B. Cornils, C.D. Frohning, C.W. Kohlpaintner, J. Mol. Catal. A 104 (1995) 17.
[9] S. Shimizu, S. Shirakawa, Y. Sasaki, C. Hirai, Angew. Chem. Int. Ed. Engl. 39 (2000) 1256.
[10] A.M. Trzeciak, J.J. Ziólkowski, Coor. Chem. Rev. 190–192 (1999) 883.
[11] S. Bischoff, M. Kant, Catal. Today 66 (2001) 183.
[12] M.E. Davis, Chemtech 22 (1992) 498.
[13] M.S. Anson, M.P. Leese, L. Tonks, J.M.J. Williams, J. Chem. Soc., Dalton Trans. (1998) 3529.
[14] J.P. Arhancet, M.E. Davis, J.S. Merola, B.E. Hanson, J. Catal. 121 (1990) 327.
[15] J.P. Arhancet, M.E. Davis, B.E. Hanson, J. Catal. 129 (1991) 94.
[16] J.P. Arhancet, M.E. Davis, B.E. Hanson, J. Catal. 129 (1991) 100.
[17] G. Fremy, E. Monflier, J.F. Carpentier, Y. Castanet, A. Mortreux, Angew. Chem. Int. Ed. Engl. 34 (1995) 1474.
[18] G. Fremy, E. Monflier, J.F. Carpentier, Y. Castanet, A. Mortreux, J. Catal. 162 (1996) 339.
[19] I.T. Horváth, Catal. Lett. 6 (1990) 43.
[20] Y. Yuan, J. Xu, H. Zhang, K. Tsai, Catal. Lett. 29 (1994) 387.
[21] T. Malmström, C. Andersson, J. Hjortkjær, J. Mol. Catal. A 139 (1999) 139.
[22] A.J. Sandee, V.F. Slagt, J.N.H. Reek, P.C.J. Kamer, P.W.N.M. van Leeuwen, Chem. Commun. (1999) 1633.
[23] I. Tóth, I. Guo, B.E. Hanson, J. Mol. Catal. A 116 (1997) 217.
[24] Y.Z. Yuan, Y.Q. Yang, J.L. Xu, H.B. Zhang, K.R. Tsai, Chin. Chem. Lett. 5 (1994) 291.
[25] P. Kalck, L. Mequel, M. Desoudeix, Catal. Today 42 (1998) 431.
[26] M. Dessoudeix, U.J. Jáuregui-Haza, M. Heughebaert, A.M. Wilhelm, H. Delmas, A. Lebugle, P. Kalck, Adv. Synth. Catal. 344 (2002) 406.
[27] U.J. Jáuregui-Haza, R. Nikolova, A.M. Wilhelm, H. Delmas, I. Nikov, Bulg. Chem. Commun. 34 (2002) 64.
[28] Y. Yuan, H. Zhang, Y. Yang, Y. Zhang, K. Tsai, Catal. Today 74 (2002) 5.
[29] I. Guo, B.E. Hanson, I. Tóth, M.E. Davis, J. Mol. Catal. 70 (1991) 363.
[30] I. Guo, B.E. Hanson, I. Tóth, M.E. Davis, J. Organomet. Chem. 403 (1991) 221.
[31] T. Bartik, B. Bartik, I. Guo, B.E. Hanson, J. Organomet. Chem. 480 (1994) 15.
[32] P. Kalck, M. Dessoudeix, Coor. Chem. Rev 190–192 (1999) 1185.
[33] J.P. Archancet, M.E. Davis, B.E. Hanson, Catal. Lett. 11 (1991) 129.
[34] K.T. Wan, M.E. Davis, J. Catal. 148 (1994) 1.
[35] S. dos Santos, Y. Tong, F. Quignard, A. Choplin, D. Sinou, J.P. Dutasta, Organometallics 17 (1998) 78.
[36] U.J. Jáuregui-Haza, M. Dessoudeix, P. Kalck, A.M. Wilhelm, H. Delmas, Catal. Today 66 (2001) 297.
[37] W.A. Herrmann, R. Manetsberger, C. Kohlpaintner, H. Bahrmann, US Patent No. 5,312,951 (May 17, 1994);
W.A. Herrmann, C.W. Kohlpaintner, R.B. Manetsberger, H. Bahrmann, H. Kottmann, J. Mol. Catal. A. 97 (1995) 65.
[38] H. Bahrmann, K. Bergrath, H.J. Kleiner, P. Lappe, C. Naumann, D. Peters, D. Regnat, J. Organomet. Chem. 520 (1996) 97;
H. Bahrmann, H. Bach, C.D. Frohning, H.J. Kleiner, P. Lappe, D. Peters, D. Regnat, W.A. Herrmann, J. Mol. Catal. A 116 (1997) 49.
[39] A. Breque, F. Mathey, P. Savignac, Synthesis (1981) 983.
[40] F. Mathey, F. Mercier, C. Charrier, J. Am. Chem. Soc. 103 (1981) 4595.
[41] W.A. Hermann, C.W. Kohlpaintner, Inorg. Synth. 32 (1998) 9.
[42] B. Heinrich, Y. Chen, J. Hjortkjær, J. Mol. Catal. 80 (1993) 365.
[43] F. Mathey, Chem. Rev. 88 (1988) 429.
[44] T. Bartik, B. Bartik, B.E. Hanson, T. Glass, W. Bebout, Inorg. Chem. 31 (1992) 2667.
[45] M. Hunger, U. Schenk, M. Breuninger, R. Gläser, J. Weitkamp, Micropor. Mesopor. Mater. 27 (1999) 261.

[46] C.W. Kohlpainter, R.W. Fischer, B. Cornils, Appl. Catal. A 221 (2001) 219.
[47] W.A. Herrmann, J.A. Kulpe, W. Konkol, H. Bahrmann, J. Organomet. Chem. 389 (1990) 85.
[48] B.B. Bunn, T. Bartik, B. Bartik, W.R. Bebout, T.E. Glass, B.E. Hanson, J. Mol. Catal. 94 (1994) 157.
[49] V.K. Likholobov, B.L. Moroz, in: G. Ertl, H. Knözinger, J. Weitkamp (Eds.), Handbook of Heterogeneous Catalysis, Chapter 4.5, vol. 4, VCH, Weinheim, 1997, p. 2231.
[50] Calculated using the software SPARTAN SGI Version 5.1.3 X11, Wavefunction Inc., USA, 1998.
[51] H. Livbjerg, K.F. Jensen, J. Villadsen, J. Catal. 45 (1976) 216.